Effects of vitamin D deficiency and supplementation on coronary and carotid arteries in rodent model

Ph.D. thesis

Hicham Dalloul MD

Doctoral School of Clinical Medicine
Semmelweis University

Supervisor: Szabolcs Várbíró MD, DSc
Marianna Török, MD, PhD

Official reviewers: Ágnes Jermendy, MD, PhD.
Ádám Lelbach, MD, med.habil

Head of the Complex Examination Committee:
Péter Várnai, MD, DSc

Members of the Final Examination Committee:
Zsolt Kopa, MD, PhD
Gábor Vermes MD, PhD

Budapest, 2022

1. Introduction

It is now a hundred years since McCollum first used the term ‘vitamin D’ in 1922. Since then, vitamin D was known as a regulator and key molecule of calcium metabolism in the human body. Beyond its skeletal effects, the role of vitamin D has been confirmed in numerous different biochemical processes and diseases. Observational studies confirm linkage of vitamin D deficiency with hypertension and major adverse cardiovascular events. We should also mention that the role of vitamin D supplementation in reducing these risks is doubtful based on the literature data. The description of the hemodynamically advantageous course and branches of the vessels can be traced back to the rules described by Murray et al. The micro preparation of intramural resistance coronary artery networks and the technique of video microscopy created the possibility to study a vascular network system in its complexity, according to these laws. In one of our studies, we sought the answer to how vitamin D deficiency can change the geometry and branching of the left anterior descending artery network.

The cerebrovascular consequence of vitamin D deficiency may also be influenced by sex. Carotid arterial function plays an important role in the regulation of cerebral blood flow and systemic blood pressure by influencing the sensitivity of the high-pressure baroreceptor reflex. In our other study, our aim was to examine the possible sex-specific effect of vitamin D deficiency on carotid arteries of rats.

2. Objectives

Cardiovascular-related deaths, hypertension and myocardial ischemia are associated with vitamin D deficiency. Both coronary arteries and carotid arteries play an important role in the cardiovascular health. In our studies we investigated how vitamin D deficiency can modify the geometry, segments and

branching of the LAD coronary artery network analyzed by video microscopy technique. Furthermore, how vitamin D deficiency affects the vasoconstrictive response of the carotid artery using wire-myographyand what sex differences are found in this process. In this dissertation I sought the answer for the following questions:

1) Are dietary alterations of vitamin D can change the geometry, branching, and distribution of arteries of different diameters of the LAD network in rodent model?

2) Are there any sex-specific differences in the contractility of the carotid artery associated with different serum vitamin D levels?

3) If there are, are these effects comes with related sex-specific alterations of the histological structure of the carotid arteries of the rat?

3. Methods

3.1. Animals

The study was designed and performed based on the Guide for the Care and Use of Laboratory Animals published by the US National Institutes of Health (8th edition, 2011) and the European Union (Directive No. 2010/63/EU). All procedures were approved by the Ethical Committee of Hungary for Animal Experimentation and University authorities (permission number: IRB: 8/2014 PEI/001/1548-3/2014, PEI/001/820-2/2015). For coronary mapping 4 weeks old male Wistar rats were randomly divided into male vitamin D deficient (MVD−, n=10) and male vitamin D supplemented (MVD+, n=8) study groups. For carotid artery measurement rats were randomly assigned to female vitamin D supplemented (FVD+, n=11-13) female vitamin D deficient (FVD−, n=11-13), male vitamin D supplemented (MVD+, 11-13) and male vitamin D deficient (MVD−, n=11-13) groups.

3.2. Treatment

During the 8 weeks long chronic treatment period, rats were housed at relative humidity of 40-70%, room temperature of 22°C ± 1°C and light-dark cycle of 12-hours each. The animals were provided different laboratory rat chow and tap water ad libitum as follows. Vitamin deficiency was induced by a vitamin D free diet (<5 IU/kg Vitamin D3, Vitamin D Free Lab Rat/Mouse Chow, Ssniff Spezialdiäten GmbH, Soest, Germany) 8 weeks (the average 25-OH-D3 level at the end of chronic treatment: 3.59 ± 0.21 ng/mL) Animals of vitamin D supplemented groups were fed by a standard laboratory diet (1000 IU/kg of Vitamin D) for 8 weeks. Oral administration (through a gavage cannula) of additional Vitamin D was given for these groups as follows: 500 IU cholecalciferol on week 2, and weeks 4,5,6,7 and 8, weekly dose of 140 IU/100g (the average 25-OH-D3 level at the end of chronic treatment: 19.66 ± 0.81 ng/mL). After 8 weeks, rats were anesthetized with Nembutal (45 mg/kg intraperitoneal (i.p.)). Biometric data were measured, the heart and carotid arteries of the animals were taken out and prepared for further analysis.

3.3. The coordinate system and geometric analysis

After taking out the heart the LAD coronary artery network was prepared by careful microdissection in cold Krebs-Ringer solution. The segments of the LAD remained intact and branches larger than 80 μm became visible. After cannulation of the orifice, the network of the LAD was perfused with nKR solution (pH=7.4, 37°C, bubbled with O_2 20%, CO_2 5% and N_2 75%) at close to in vivo pressures. Photos of the coronary network was recorded by a video-microscope using different magnifications (low and high magnifications, 8.58 and 1.47 μm/pixel). For analyzation we used the ImageJ software, NIH, Bethesda, MA, USA. Pictures taken from perpendicular position were selected to rebuild a horizontally stretched network for analysis. A coordinate system was created, the X-axis was drawn between

the orifice and the apex of the heart. The Y-axis was erected perpendicularly to the X-axis, putting positive values in the direction of the left ventricle. The zero point for both axes was the orifice. Segments were divided into 50 micrometer long cylindrical units, diameter, direction, and coordinate position of all components were determined.

3.4. Segment analysis

The whole network has been divided into segments. Length, outer and inner vessel diameters of the segments were measured. From the inner radius (ri) data, the lumen cross section area was calculated according to the following formula:

Lumen cross section area (μm^2) = ri^2 * Π

Distances of the branching points from origin, angles of two related segments segmental axes and angles with the coordinate were also analyzed. Direct distance of bifurcations, segments, ring units from the orifice was computed. In addition, for each segment, a length for the potentially curved axis was also computed. This way "flow distances" from the orifice or for the segments could be compared with direct distances, giving an opportunity to calculate the tortuosity of the network

3.5. Branching analysis

All bifurcations were sorted into dichotomic, multiplex or lateral branching categories. All bifurcations were tested for the validity of Murray's law: $Dom^3 = Dod1^3 + Dod2^3$ where Do is the outer diameter in μm, m, d1 and d2 are the mother and daughter branches. The asymmetry index (Ai) was calculated according to the following formula: $Ai = Dod1 / Dod2$ where Do is the outer diameter in μm, d1 and d2 are the daughter branches (the data of the larger daughter branch was always put in the numerator/top).

3.6. Analysis of 50 μm long vascular ring units

Theoretically, all coronary artery networks were divided into 50 μm long ring units. The ring units were located in the X-Y

coordinate system. The outer and inner diameter, wall thickness, X and Y coordinates for the ring unit center, angle of axis with the X-axis, flow distance and the direct distance from the orifice were measured. The ring unit analysis was performed by constructing lists of ring units in certain inner/outer diameter range, in certain direct/flow distance from the orifice.

3.7. Network anomalies

Parallel running branches, broken course, multiple branching e.g., triple) present in the systems were counted. Tortuosity and asymmetric branching proportions (Ai>2) were measured. Tortuosity (T), curvature, ratios of segments were computed comparing the direct distance between the start and end points of the segment as well as the potentially curved length of the segment's axis following the route of blood flow:

T(%) = 100 – (segment length in the airline (µm) * 100 / segment length in real (µm)).

3.8. Wire myography

Carotid arterial segments were cut into 2 mm long rings and placed on a conventional wire myograph setup (610-M MultiMyograph System, Danish Myo Technology, Aarhus, Denmark, with Lab-Chart Evaluation System, AD Instruments, Oxford, UK–Ballagi LTD, Budapest, Hungary). The organ chambers were filled with 8 ml nKR solution to maintain stable pH. The contractility of the vessels was obtained when applying 124 mmol/L K+, which served as the reference value of the contraction forces. Vascular rings were equilibrated in nKR, and accumulative doses of phenylephrine (10−9–10−6 mol/L) were administrated to induce contraction. Measurements was repeated in the presence of the nitric oxide synthase inhibitor N(G)-Nitro-L-arginine methyl ester (L-NAME) (10−4 mol/L) and the general COX inhibitor indomethacin (10−5 mol/L) or their vehicle DMSO.

3.9 Immunohistochemistry

A vascular ring of carotid arteries was fixed in formaldehyde and embedded in paraffin. Carotid arterial tissue sections were stained with resorcin-fuchsin (RF). Immuno-histochemistry was performed to label alpha smooth muscle actin (SMA), thromboxane A2 receptor (TP) and 3-nitrotyrosin (NT). Antigen retrieval was performed by heating the slides in citrate buffer (pH = 6) following deparaffinization. Then, 3% H_2O_2 in dH_2O was applied to block endogenous peroxidase activity. Non-specific labeling was prevented via utilization of 2.5% normal horse serum. Primary antibodies (SMA: 1:10000; TP 1:50 and NT 1:500) were applied overnight at 4 °C. For SMA horseradish-peroxidase-linked anti-mouse was used for secondary labeling, while for TP and NT anti-rabbit polyclonal horse antibody was used for secondary labeling. Visualization of specific labeling was accomplished by brown-colored diamino-benzidine (DAB), while blue-colored hematoxylin served for counterstaining. Brightfield microscopy images were acquired using a Nikon ECLIPSE NI-U microscope and Nikon DS-Ri2 camera (Nikon, Minato City, Tokyo, Japan) with 40x objective. Non-calibrated optical density of the media layer of resorcin-fuchsin-stained vessels was obtained for the purpose of assessing the density of non-contractile elements using ImageJ software (National Institutes of Health (NIH), Bethesda, MA, USA). The measurements of the non-calibrated optical density of specific staining in the intimal or medial layers of the vessel wall were also completed with ImageJ software in the case of immunohistochemical labeling.

3. Statistical analysis

GraphPad Prism 5, SPSS Sigma Stat and Excel software were used for statistical analysis. All data are presented as mean ± SEM. In the case of normal distribution (tested using the Shapiro-Wilk method), the two-tailed unpaired Student’s t-test was performed. The Mann-Whitney test was performed, in the

case of non-normal distribution. Morphological abnormalities were counted and pooled and normalized in 8 rats for all perfused networks. Their number was tested with the test. Frequencies of ring unit in different diameter ranges in MVD+ and MVD− coronary networks were compared with the $\chi 2$ test. Pearson correlation method was used to evaluate interconnection between bifurcations asymmetry and angle. A 3D scatter plot was used to show differences in bifurcation ranch angle as a function of vessel diameter. The level of deviation of flow route from direct distance from orifice and diameter of the ring were analyzed on 3D plots of two-dimensional histograms. Number of ring units in a given diameter and flow distance range was analyzed in two dimensional histograms and visualized in 3D (color coded) maps. Repeated measures two-way ANOVA was completed using Bonferroni's post hoc test for the analysis of vascular function curves. At a certain agonist concentration, vascular reactivity was analyzed by two-way ANOVA (sex, vitamin D status). The Kruskal–Wallis's test with Dunn's multiple comparison test was applied to accomplish the comparison of histological and immunohistochemical evaluations of the experimental groups. $p < 0.05$ was used as the criterion for statistical significance.

4. Results

4.1 Coronary artery mapping

4.1.1. Biometric data. Body and heart weight, arterial blood pressure

Vitamin D deficiency and supplementation for 8 weeks long therapy did not affect the biometric data. Differences of body weight (MVD−: 481±15 vs. MVD+: 477±19 g), heart weight (MVD−: 1.37±0.04 vs. MVD+: 1.32±0.08 g) and blood pressure observed invasively by measuring it in the right carotid artery (MVD−: 95.39±4.35 vs. MVD+: 88.18±6.57 mmHg) did not show any significant alteration between the two groups

4.1.2. Segments analysis

The segments and branching of coronary resistance showed no difference between the study groups (MVD−: 210 and MVD+: 224 segments, normalized in 8 animals). Significantly larger lumen surface area of the primary branches found in the MVD+ group (MVD−: 112554±12961 vs. MVD+: 167593±24108, Two-tailed unpaired Student's t-test, p=0.046). Lumen diameters did not differ during the next branching steps. Segments of order 1 (MVD−: 1954±223 vs. MVD+: 1211±63, Mann-Whitney-test, p=0.0266) and 4 (MVD−: 2064±254 vs. MVD+: 1538±240, Mann-Whitney-test, p=0.0087) were significantly, 2 and 3 were slightly longer in MVD− rats. Interestingly, branches of 11-12 order were showed up only in the VD+ group.

4.1.3. Analyzes of the branches

One of the guiding principles of microvascular geometry is that smaller branches deviate more from the axis of the main branch than larger secondary branches. Analyzing the vitamin D substituted networks, this is clearly visible, although is lacking in vitamin D deficient animals. (**Fig**. **1A**, significant by Pearson correlation). **Figure 1B** shows that the bifurcation of the study groups was met the criterion exactly of Murray's law.

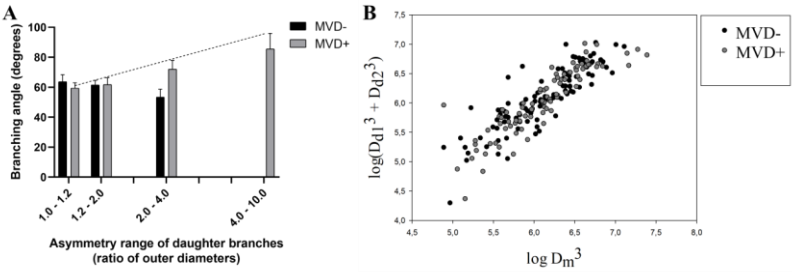

Figure 1. Analysis of branching (A) Range of asymmetry of the secondary branches (ratio of outer diameters). ($p<0.05$ Pearson correlation, Values are means ± SEM). n=10 in MVD− and n=8 in MVD+). (B) The Murray's law. Branching is obeying the Murray's law.

4.1.4. Abnormalities

Vitamin D deficiency did not change the amount of morphological deviation such as parallel running, track breakage, multiple segments branching, or vessel tortuosity (sum of all deformities MVD−: 27 vs. MVD+: 22, Chi2 probe, n.s.).

4.1.5. 50 μm long cylindrical ring unit analysis

MVD+ animals had a slightly richer coronary resistance arterial network compared with MVD− rats **(Fig. 2)**.

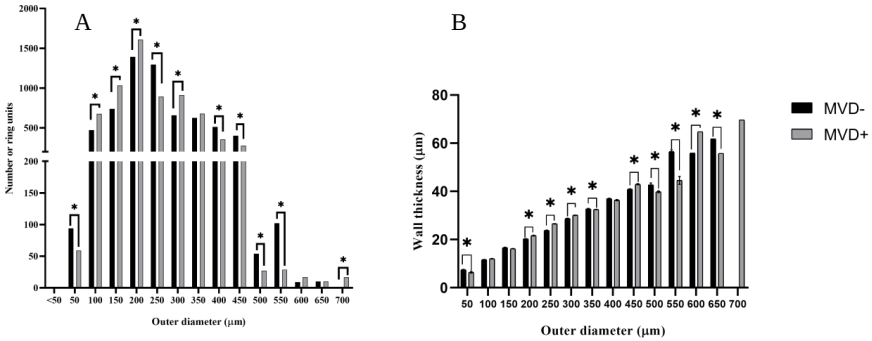

Figure 2. Analysis of ring units (A) Number of 50 μm ring units as a function of different diameter ranges. Normalized for 8-8 rats. Significantly different with the Chi2(X^2) probe ($p<0.05$). (B) Wall thickness of 50 μm ring units as a function of different diameter ranges. Values are means ± SEM. n=10 in MVD− and n=8 in MVD+. Mann-Whitney-test. *P<0.05 MVD− vs. MVD+.

Dividing the entire network into ring units of 50 μm, there were significantly fewer such units in MVD− group. (6365 vs. 6602, overall data, normalized to 8 study animals with a $p < 0.0374$ $\chi 2$ probe). **Fig. 2A** shows that in MVD+ animals, increased number of vascular units was present in the outer diameter range of 100–300 μm. MVD− animals had significantly more larger diameter ring units in the range of 400–550 μm. At the same time at this range of diameter the ring units showed wall thickening. Thickness of the vessel wall thickening was bigger in MVD+ animals in the most common diameter range of 200–300 μm

(Fig. 2B). The heat-map histogram in **Fig. 3** shows that a new population of 250 μm diameter ring units appears at a flow distance of 6-9 mm from the orifice in vitamin D deficient animals, while a decrease of 350 μm is observed at the same sites. In vitamin D deficient rats, units of 150-200 and 300 μm are almost absent at a flow distance of 10–15 mm.

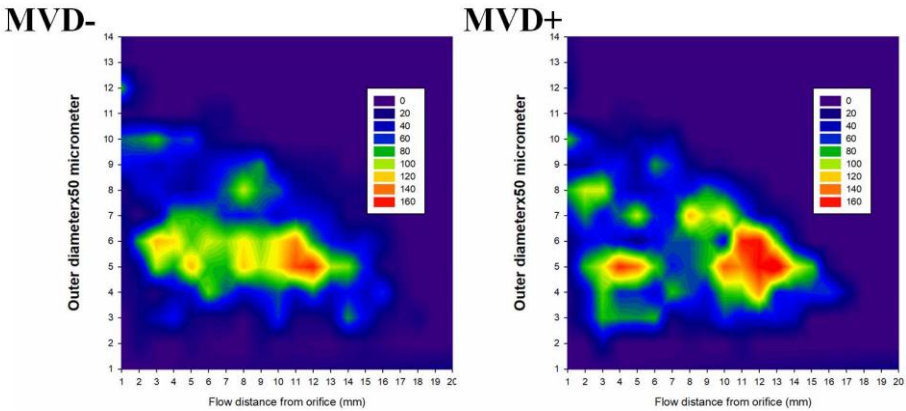

Figure 3. Frequency of ring unit (color coded) for different diameters and flow distances from the orifice

4.2. Carotid Arteries

4.2.1. Phenylephrine-Induced Contraction of Carotid Arteries

Sex alterations in phenylephrine-induced contraction can be seen at phenylephrine concentrations of 10^{-6} mol/L male rats showed stronger contraction, regardless of the status of serum vitamin D level. In general, vitamin D deficiency resulted in more pronounced contractions induced by phenylephrine **(Fig. 4A)**. At phenylephrine concentrations of 10^{-7} mol/l, carotid arteries of male, vitamin D deficient rats showed an enhanced contraction compared to female animals. In addition, female arteries from the vitamin D supplemented study group showed decreased contraction. At a phenylephrine concentration of 10^{-6} mol/l, the carotid arteries of male rats from the supplemented

group showed decreased contraction than vessels of male rats with vitamin D deficiency **(Fig. 4B)**. To elucidate the role of endothelial nitric oxide synthase and cyclooxygenases, in phenylephrine-induced contractions, the study was repeated in the presence of L–NAME and indomethacin and their combination. L-NAME forced the contraction in all study subgroups. However, indomethacin did not alter the reactivity in the presence of L-NAME in most groups, except for vitamin D-deficient males, where it further enhanced the contraction compared with the effect of L-NAME alone.

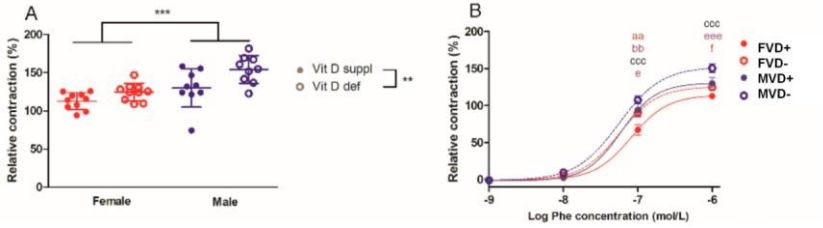

Figure 4. Contraction ability of isolated carotid artery segments (A) phenylephrine (Phe)-induced contraction in the four experimental groups at 10^{-6} mol/L Phe concentration. Data are shown as individual data points; horizontal lines represent mean ± SEM Two-way ANOVA; factors: sex, vitamin D status. **: $p < 0.01$, ***: $p < 0.001$. (B) Phe-induced contraction. Data are shown as mean ± SEM; n = 9–11 in each group; repeated measures ANOVA, Bonferroni's post hoc test; aa: $p < 0.01$ FD+ vs. FD−, bb: $p < 0.01$ FVD+ vs. MVD+, ccc: $p < 0.001$ FVD+ vs. MVD−, e: $p < 0.05$ FVD− vs. MVD−, eee: $p < 0.001$ FVD− vs. MVD−, f: $p < 0.05$ MD+ vs. MVD−.

Indomethacin reduced the force of contraction only in female vitamin D-supplemented rats, which suggests that astringent prostanoids play a significant role in these animals **(Fig. 5A – D)**. The lack of effect of indomethacin in male, vitamin D-supplemented and female vitamin D deficient study groups suggest sex- and vitamin D dependent regulation of prostanoid induced vasoconstriction.

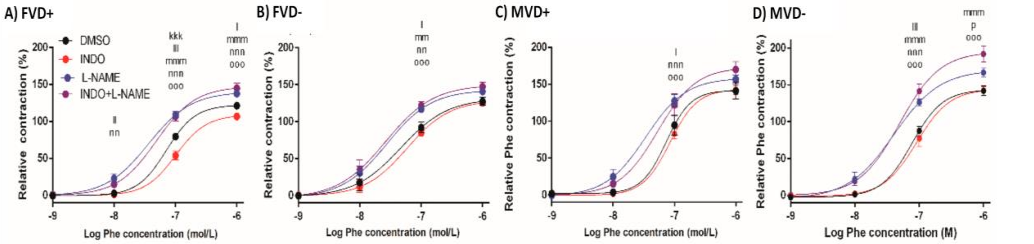

Figure 5. Contraction ability of isolated carotid artery segments in the presence of inhibitors Phe-induced contractions in the presence of L-NAME and/or indomethacin (INDO) or their vehicle DMSO (A) in female vitamin D supplemented rats (FVD+) (B) in female vitamin D deficient rats (FVD−), (C) in male vitamin D supplemented rats (MVD+) and (D) in male vitamin D deficient rats (MVD−). Data are shown as mean ± SEM; n = 5–11 in each group; repeated measures ANOVA, Bonferroni's post hoc test; kkk: $p < 0.001$ DMSO vs. INDO, l: $p < 0.05$ DMSO vs. L-NAME, lll: $p < 0.001$ DMSO vs. L-NAME, mm: $p < 0.01$ DMSO vs. INDO+L-NAME, mmm: $p < 0.001$ DMSO vs. INDO+L-NAME, nn: $p < 0.01$ INDO vs. L-NAME, nnn: $p < 0.001$ INDO vs. L-NAME, ooo: $p < 0.001$ INDO vs. INDO+L-NAME, p: $p < 0.05$ L-NAME vs. INDO+L-NAME .

4.2.2. Vitamin D status and sex induced histological alterations of the Carotid Arteries

Vitamin D deficiency decreased the number of elastic fibers in isolated carotid arteries of female animals significantly in but not in males. What can be a result of the marked, but not significant decrease of elastic fiber staining of the male carotid arteries **(Fig. 6A)**. On the other hand, vitamin D deficiency decreased the staining intensity observed after smooth muscle actin (SMA) immunolabeling of carotid arteries of male animals. This change cannot be seen in females **(Fig. 6B)**. Thromboxane A2 receptor (TP) showed a marked increase of immunopositivity induced by vitamin D deficiency in male animals but not in females **(Fig. 6C)**. Nitrative stress characterized by tyrosine nitration was less strong in both male groups compared to female vitamin D deficient animals **(Fig. 6D)**.

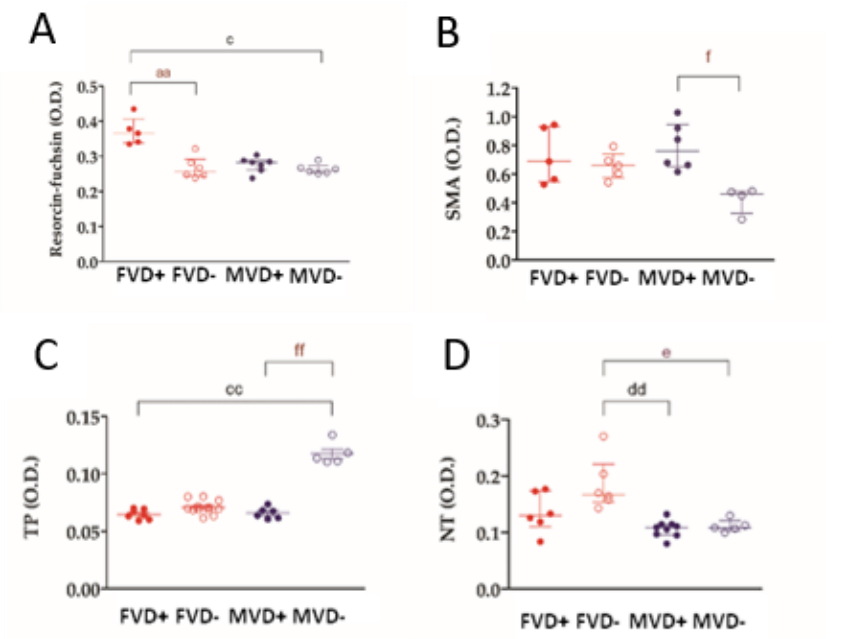

Figure 6. Histological changes of the carotid arteries (A) Elastic fiber density of carotid artery segments. (B) Alpha smooth muscle actin (SMA) immunohistochemical labelling intensity in the media layer of carotid arteries. (C) Thromboxane A2 receptor (TP) density of carotid arteries. (D) 3-Nitrotyrosine (NT) staining intensity of carotid arteries. Scale bars show 50 µm. Data are presented as individual data points and lines represent the median (IQR); Kruskal–Wallis test with Dunn's post hoc test; aa: $p < 0.01$ FVD+ vs. FVD−, c: $p < 0.05$ FVD+ vs. MVD−, cc: $p < 0.01$ FVD+ vs. MVD−, dd: $p < 0.01$ FVD− vs. MVD+, e: $p < 0.05$ FVD− vs. MVD−, f: $p < 0.05$ MVD+ vs. MVD−, ff: $p < 0.01$ MVD+ vs. MVD− .

5. Conclusions

Our experiments focused on the following questions:

1) Do dietary alterations of vitamin D and the effects of serum vitamin D alterations can change the formation of the complex geometry of the left anterior descending coronary artery (LAD) network in rodent model? Do the branching and segments property change? Does the distribution of cylindrical ring units of arteries of different diameters show alteration?

Although there are no network abnormalities or difference of the number of segments found, several alterations of the LAD system occurred associated with serum vitamin D levels. An increase in the wall thickness of larger segments, a decrease in the number of smaller-diameter ring elements, and changes in bifurcation angles in different study groups indicate some involvement of vitamin D in the morphological development of coronary artery networks. Thus, due to the richer network created by vitamin D supplementation may improves tissue perfusion. In the vitamin D supplemented animals, the networks were richer, the branching pattern was optimal, with no abnormalities. While these can only be expected to have moderate hemodynamic effects, they may can alter pathological processes.

2) Are there any sex-specific differences in the contractility of the carotid artery associated with different serum vitamin D levels?

Low vitamin D levels such as male sex caused enhanced contractile properties of carotid arteries of the rats. The shifting balance of circulating plasma prostanoid levels increases the effect of vasoconstriction in male rats in the presence of L-NAME. This can be a result of the histologic alterations of TP immunostaining of the males. COX inhibition alone leads to a decrease in Phe-induced contraction in vitamin D supplemented female rats, which can not be seen in vitamin D deficiency. Although does not affect the contraction of the carotid arteries of the male rats

3) If there are, are these effects comes with related sex-specific alterations of the histological structure of the carotid arteries of the rat?

Changes of the contractility of the carotid arteries induced by vitamin D alterations apply together with sex-specific histological alterations. Staining of elastic fibers became fainter as a result of the vitamin D deficiency in female animals, but not

in male rats. Smooth muscle actin staining increased, the thromboxane receptor staining showed a marked increase in the male vitamin D deficient group. Decreased nitrative stress level based on the histology remained lower in both male groups regardless from VD supply.

6. Bibliography of the candidate's publications

Publications related to the thesis:

Sipos Miklós*, Gerszi D, Dalloul H*, Bányai B, Sziva RE, Kollarics R, Magyar P, Török M, Ács N, Szekeres M, Nádasy GyL, Hadjadj L, Horváth EM, and Várbíró Szabolcs. Vitamin D deficiency and sex alter vasoconstrictor and vasodilator reactivity in rat carotid artery. INTERNATIONAL JOURNAL OF MOLECULAR SCIENCES. 2021
Impact factor: 6,208

Dalloul H, Hainzl T, Monori-Kiss A, Hadjadj L, Nádasy GL, Török M, and Várbíró Szabolcs. Vitamin-D Deficiency and Supplementation Altered the Network of the Coronary Arteries in a Rodent Model — In Situ Video Microscopic Technique. NUTRIENTS. 2022
Impact factor: 6,706

Publications not related to the thesis:

Costa A, Dalloul H, Hegyesi H, Apor P, Csende Z, Racz L, Vaczi M, and Tihanyi József. Impact of repeated bouts of eccentric exercise on myogenic gene expression. European JOURNAL OF APPLIED PHYSIOLOGY. 2007
Impact factor: 1,752

Karászi É, Onozó B, Sütő A, Kutas K, Szalóczi B, Laczkovszki M, Demeter G, Kovács F, Tordas D, Dalloul H, Világos E, Erlaky H. Clinical and epidemiological characteristics of pediatric COVID-19 patients in a community-based study. ORVOSI HETILAP. 2021
Impact factor: 0,540

Dalloul H, Eszméletvesztés és syncope a gyermekorvosi gyakorlatban. Vezérfonal az alapellátók számára GYERMEKGYÓGYÁSZAT. 2021

∑IF: 15,206